SIAM J. NUMER. ANAL.
Vol. 41, No. 4, pp. 1406–1426

AN EXPLICIT UNCONDITIONALLY STABLE NUMERICAL METHOD FOR SOLVING DAMPED NONLINEAR SCHRÖDINGER EQUATIONS WITH A FOCUSING NONLINEARITY*

WEIZHU BAO† AND DIETER JAKSCH‡

Abstract. This paper introduces an extension of the time-splitting sine-spectral (TSSP) method for solving damped focusing nonlinear Schrödinger equations (NLSs). The method is explicit, unconditionally stable, and time transversal invariant. Moreover, it preserves the exact decay rate for the normalization of the wave function if linear damping terms are added to the NLS. Extensive numerical tests are presented for cubic focusing NLSs in two dimensions with a linear, cubic, or quintic damping term. Our numerical results show that quintic or cubic damping always arrests blowup, while linear damping can arrest blowup only when the damping parameter δ is larger than a threshold value $\delta_{\rm th}$. We note that our method can also be applied to solve the three-dimensional Gross–Pitaevskii equation with a quintic damping term to model the dynamics of a collapsing and exploding Bose–Einstein condensate (BEC).

Key words. damped nonlinear Schrödinger equation (DNLS), time-splitting sine-spectral (TSSP) method, Gross–Pitaevskii equation (GPE), Bose–Einstein condensate (BEC), complex Ginzburg–Landau (CGL)

AMS subject classifications. 35Q55, 65T40, 65N12, 65N35, 81-08

DOI. 10.1137/S0036142902413391

1. Introduction.

Since the first experimental realization of Bose–Einstein condensation (BEC) in dilute weakly interacting gases, the nonlinear Schrödinger equation (NLS) has been used extensively to describe the single particle properties of BECs. The results obtained by solving the NLS showed excellent agreement with most of the experiments (for a review, see [2, 3, 11, 10]). In fact, up to now there have been very few experiments in ultracold dilute bosonic gases which could not be described properly by using theoretical methods based on the NLS [20, 23].

Recent experiments by Donley et al. [12] provide new experimental results for checking the validity of describing a BEC by using the NLS in the case of attractive interactions (focusing nonlinearity) in three dimensions. Since the particle density might become very large in the case of attractive interactions, inelastic collisions become important and cannot be neglected. These inelastic collisions are assumed to be accounted for by adding damping terms to the NLS. Two particle inelastic processes are taken into account by a cubic damping term, while three particle inelastic collisions are described by a quintic damping term. Collisions with the background gas and feeding of the condensate can be studied by adding linear damping terms. One of the major theoretical challenges in comparing results obtained in the experiment with theoretical results is to find reliable methods for solving the NLS with a focusing

*Received by the editors August 25, 2002; accepted for publication (in revised form) January 31, 2003; published electronically September 9, 2003. This work was supported by the WITTGENSTEIN-AWARD of P. Markowich and P. Zoller which is funded by the Austrian National Science Foundation FWF.

http://www.siam.org/journals/sinum/41-4/41339.html

†Department of Computational Science, National University of Singapore, Singapore 117543 (bao@cz3.nus.edu.sg). The research of this author was supported by National University of Singapore grant R-151-000-027-112.

‡Institut für Theoretische Physik, Universität Innsbruck, A-6020 Innsbruck, Austria (dieter.jaksch@physics.oxford.ac.uk).

nonlinearity and damping terms in the parameter regime where the experiments are performed.

The aim of this paper is to extend the time-splitting sine-spectral (TSSP) method for solving the focusing NLS with additional damping terms and to present extensive numerical tests. The comparison of our numerical results with the experimental results obtained for a collapsing BEC [12] will be presented elsewhere [8].

We consider the NLS [7, 36]

$$i\,\psi_t = -\frac{1}{2}\,\Delta\psi + V(\mathbf{x})\,\psi - \beta|\psi|^{2\sigma}\psi, \qquad t>0, \qquad \mathbf{x}\in\mathbb{R}^d, \tag{1.1}$$

$$\psi(\mathbf{x}, t=0) = \psi_0(\mathbf{x}), \qquad \mathbf{x}\in\mathbb{R}^d, \tag{1.2}$$

with $\sigma > 0$ a positive constant, where $\sigma = 1$ corresponds to a cubic nonlinearity, $\sigma = 2$ corresponds to a quintic nonlinearity, $V(\mathbf{x})$ is a real-valued potential whose shape is determined by the type of system under investigation, and β positive/negative corresponds to the focusing/defocusing NLS. In BEC, where (1.1) is also known as the Gross–Pitaevskii equation (GPE) [21, 26, 33], ψ is the macroscopic wave function of the condensate, t is time, $\mathbf{x}$ is the spatial coordinate, and $V(\mathbf{x})$ is a trapping potential which usually is harmonic and can thus be written as $V(\mathbf{x}) = \frac{1}{2}\left(\gamma_1^2 x_1^2 + \cdots + \gamma_d^2 x_d^2\right)$ with $\gamma_1, \ldots, \gamma_d \geq 0$. Two important invariants of (1.1) are the *normalization of the wave function*

$$N(t) = \int_{\mathbb{R}^d} |\psi(\mathbf{x},t)|^2\, d\mathbf{x}, \qquad t\geq 0, \tag{1.3}$$

and the *energy*

$$E(t) = \int_{\mathbb{R}^d} \left[\frac{1}{2}|\nabla\psi(\mathbf{x},t)|^2 + V(\mathbf{x})|\psi(\mathbf{x},t)|^2 - \frac{\beta}{\sigma+1}|\psi(\mathbf{x},t)|^{2\sigma+2}\right] d\mathbf{x}, \quad t\geq 0. \tag{1.4}$$

From the theory for the local existence of the solution of (1.1), it is well known that if $\|\psi(\cdot,t)\|_{H^1}$ is bounded, the solution exists for all t [36]. As a result, when the NLS is defocusing ($\beta < 0$), conservation of energy implies that $\int_{\mathbb{R}^d} |\nabla\psi(\mathbf{x},t)|^2\, d\mathbf{x}$ is bounded and the solution exists globally. On the other hand, if the NLS is focusing ($\beta > 0$) at critical ($\sigma d = 2$) or supercritical ($\sigma d > 2$) dimensions and for an initial energy $E(0) < 0$, then the solutions of (1.1) can self-focus and become singular in finite time; i.e., there exists a time $t_* < \infty$ such that (see [36])

$$\lim_{t\to t_*} |\nabla\psi|_{L^2} = \infty \qquad \text{and} \qquad \lim_{t\to t_*} |\psi|_{L^\infty} = \infty.$$

However, the physical quantities modeled by ψ do not become infinite, which implies that the validity of (1.1) breaks down near the singularity. Additional physical mechanisms, which were initially small, become important near the singular point and prevent the formation of the singularity. In BEC, the particle density $|\psi|^2$ becomes large close to the critical point, and inelastic collisions between particles which are negligible for small densities become important. Therefore, a small damping (absorption) term is introduced into the NLS (1.1) which describes inelastic processes. We are interested in the cases where these damping mechanisms are important and therefore restrict ourselves to the case of focusing nonlinearities $\beta > 0$, where β may also be time dependent. We consider the damped nonlinear Schrödinger equation (DNLS)

$$i\,\psi_t = -\frac{1}{2}\,\Delta\psi + V(\mathbf{x})\,\psi - \beta|\psi|^{2\sigma}\psi - i\,g(|\psi|^2)\psi, \qquad t>0, \quad \mathbf{x}\in\mathbb{R}^d, \tag{1.5}$$

$$\psi(\mathbf{x}, t=0) = \psi_0(\mathbf{x}), \qquad \mathbf{x}\in\mathbb{R}^d, \tag{1.6}$$

where $g(\rho) \geq 0$ for $\rho = |\psi|^2 \geq 0$ is a real-valued monotonically increasing function.

The general form of (1.5) covers many DNLSs arising in various different applications. In BEC, for example, when $g(\rho) \equiv 0$, (1.5) reduces to the usual GPE (1.1); a linear damping term $g(\rho) \equiv \delta$ with $\delta > 0$ describes inelastic collisions with the background gas; cubic damping $g(\rho) = \delta_1 \beta \rho$ with $\delta_1 > 0$ corresponds to two-body loss [13, 35, 34]; and a quintic damping term of the form $g(\rho) = \delta_2 \beta^2 \rho^2$ with $\delta_2 > 0$ adds three-body loss to the GPE (1.1) [1, 35, 34]. It is easy to see that the decay of the normalization according to (1.5) due to damping is given by

$$N'(t) = \frac{d}{dt} \int_{\mathbb{R}^d} |\psi(\mathbf{x}, t)|^2 \, d\mathbf{x} = -2 \int_{\mathbb{R}^d} g(|\psi(\mathbf{x}, t)|^2) |\psi(\mathbf{x}, t)|^2 \, d\mathbf{x} \leq 0, \quad t > 0. \tag{1.7}$$

In particular, if $g(\rho) \equiv \delta$ with $\delta > 0$, the normalization is given by

$$N(t) = \int_{\mathbb{R}^d} |\psi(\mathbf{x}, t)|^2 \, d\mathbf{x} = e^{-2\delta \, t} N(0) = e^{-2\delta \, t} \int_{\mathbb{R}^d} |\psi_0(\mathbf{x})|^2 \, d\mathbf{x}, \quad t \geq 0. \tag{1.8}$$

There has been a series of recent studies which deals with the analysis and numerical solution of the DNLS. Fibich [14] analyzed the effect of linear damping (absorption) on the critical self-focusing NLS, Tsutsumi [37, 38] studied the global solutions of the NLS with linear damping, and the regularity of attractors and approximate inertial manifolds for a weakly damped NLS were given in Goubet [17, 19, 18] and by Jolly, Temam, and Xiong [24]. For numerically solving the linearly damped NLS, Peranich [32] proposed a finite difference scheme, and this method was revisited recently by Ciegis and Pakalnyte [9] and Zhang and Lu [39]. Moebs and Temam [30] presented a multilevel method for weakly damped NLS, and Moebs applied it to solve a stochastic weakly damped NLS in [29]. Variable mesh difference schemes for the NLS with a linear damping term were used by Iyengar, Jayaraman, and Balasubramanian [22].

Also, the TSSP method, which we will use in this paper to solve the DNLS, was already successfully used for solving the Schrödinger equation in the semiclassical regime and for describing BEC using the GPE by Bao et al. [4, 5, 7]. The TSSP method is explicit, unconditionally stable, and time transversal invariant. Moreover, it gives the exact decay rate of the normalization when linear damping is applied to the NLS (i.e., $g(\rho) \equiv \delta$ with $\delta > 0$ in (1.5)) and yields spectral accuracy for spatial derivatives and second-order accuracy for the time derivative. Thus this method is a very good candidate for solving the DNLS, especially in two or three dimensions. We test the novel numerical method extensively in two dimensions.

Finally, we want to emphasize that the NLS is also used in nonlinear optics, e.g., to describe the propagation of an intense laser beam through a medium with a Kerr nonlinearity [16, 36]. In nonlinear optics, $\psi = \psi(\mathbf{x}, t)$ describes the electrical field amplitude, t is the spatial coordinate in the direction of propagation, $\mathbf{x} = (x_1, \ldots, x_d)^T$ is the transverse spatial coordinate, and $V(\mathbf{x})$ is determined by the index of refraction. Nonlinear damping terms of the form $g(\rho) = \delta \beta^q \rho^q$ with $\delta, q > 0$ correspond to multiphoton absorption processes [14].

The paper is organized as follows. In section 2, we present the TSSP approximation for the damped nonlinear Schrödinger equation. In section 3, numerical tests are presented for the cubic focusing NLS in two dimensions with a linear, cubic, or quintic damping term. In section 4, some conclusions are drawn.

2. Time-splitting sine-spectral method. In this section we present a time-splitting sine-spectral (TSSP) method for solving the problem (1.5), (1.6) with homogeneous periodic boundary conditions. For simplicity of notation, we shall introduce

the method for the case of one spatial dimension ($d = 1$). Generalizations to $d > 1$ are straightforward for tensor product grids, and the results remain valid without modifications. For $d = 1$, the problem becomes

$$i\,\psi_t = -\frac{1}{2}\psi_{xx} + V(x)\psi - \beta|\psi|^{2\sigma}\psi - i\,g(|\psi|^2)\psi, \qquad a < x < b, \quad t > 0, \tag{2.1}$$

$$\psi(x, t = 0) = \psi_0(x), \quad a \le x \le b, \qquad \psi(a, t) = \psi(b, t) = \mathbf{0}, \quad t \ge 0. \tag{2.2}$$

2.1. General damping term. We choose the spatial mesh size $h = \Delta x > 0$ with $h = (b - a)/M$ and M an even positive integer. The time step is given by $k = \Delta t > 0$, and we define grid points and time steps by

$$x_j := a + j\,h, \qquad t_n := n\,k, \qquad j = 0, 1, \ldots, M, \qquad n = 0, 1, 2, \ldots.$$

Let ψ_j^n be the numerical approximation of $\psi(x_j, t_n)$ and ψ^n the solution vector at time $t = t_n = nk$ with components ψ_j^n.

From time $t = t_n$ to time $t = t_{n+1}$, the DNLS (2.1) is solved in two steps. One solves

$$i\,\psi_t = -\frac{1}{2}\psi_{xx} \tag{2.3}$$

for one time step, followed by solving

$$i\,\psi_t(x, t) = V(x)\psi(x, t) - \beta|\psi(x, t)|^{2\sigma}\psi(x, t) - i\,g(|\psi(x, t)|^2)\psi(x, t), \tag{2.4}$$

again for the same time step. Equation (2.3) is discretized in space by the sine-spectral method and integrated in time *exactly*. For $t \in [t_n, t_{n+1}]$, multiplying the ODE (2.4) by $\overline{\psi(x,t)}$, the conjugate of $\psi(x, t)$, one obtains

$$i\,\psi_t(x, t)\overline{\psi(x, t)} = V(x)|\psi(x, t)|^2 - \beta|\psi(x, t)|^{2\sigma+2} - i\,g(|\psi(x, t)|^2)|\psi(x, t)|^2. \tag{2.5}$$

Subtracting the conjugate of (2.5) from (2.5) and multiplying by $-i$, one obtains

$$\frac{d}{dt}|\psi(x, t)|^2 = \overline{\psi_t(x, t)}\psi(x, t) + \psi_t(x, t)\overline{\psi(x, t)} = -2g(|\psi(x, t)|^2)|\psi(x, t)|^2. \tag{2.6}$$

Let

$$f(s) = \int \frac{1}{s\,g(s)}\,ds, \qquad h(s, \tau) = \begin{cases} f^{-1}\left(f(s) - 2\tau\right), & s > 0,\ \tau \ge 0, \\ 0, & s = 0,\ \tau \ge 0. \end{cases} \tag{2.7}$$

Then, if $g(s) \ge 0$ for $s \ge 0$, we find

$$0 \le h(s, \tau) \le s \qquad \text{for} \quad s \ge 0, \quad \tau \ge 0, \tag{2.8}$$

and the solution of the ODE (2.6) can be expressed as (with $\tau = t - t_n$)

$$\begin{aligned} 0 \le \rho(t) = \rho(t_n + \tau) &:= |\psi(x, t)|^2 = h\left(|\psi(x, t_n)|^2, t - t_n\right) := h\left(\rho(t_n), \tau\right) \\ &\le \rho(t_n) = |\psi(x, t_n)|^2, \qquad t_n \le t \le t_{n+1}. \end{aligned} \tag{2.9}$$

Combining (2.9) and (2.4), we obtain

$$\begin{aligned} i\,\psi_t(x, t) = V(x)\psi(x, t) &- \beta\left[h\left(|\psi(x, t_n)|^2, t - t_n\right)\right]^\sigma \psi(x, t) \\ &- i\,g\left(h\left(|\psi(x, t_n)|^2, t - t_n\right)\right)\psi(x, t), \qquad t_n \le t \le t_{n+1}. \end{aligned} \tag{2.10}$$

Integrating (2.10) from t_n to t, we find

$$\psi(x,t) = \exp\left\{i\left[-V(x)(t-t_n) + G\left(|\psi(x,t_n)|^2, t-t_n\right)\right] - F\left(|\psi(x,t_n)|^2, t-t_n\right)\right\} \times \psi(x,t_n), \qquad t_n \le t \le t_{n+1}, \tag{2.11}$$

where we have defined

$$F(s,r) = \int_0^r g(h(s,\tau))\, d\tau \ge 0, \quad G(s,r) = \int_0^r \beta\ [h(s,\tau)]^\sigma\ d\tau. \tag{2.12}$$

To find the time evolution between $t = t_n$ and $t = t_{n+1}$, we combine the splitting steps via the standard second-order Strang splitting TSSP method for solving the DNLS (2.1). In detail, the steps for obtaining ψ_j^{n+1} from ψ_j^n are given by

$$\begin{aligned}
\psi_j^* &= \exp\left\{-F\left(|\psi_j^n|^2, k/2\right) + i\left[-V(x_j)k/2 + G\left(|\psi_j^n|^2, k/2\right)\right]\right\}\ \psi_j^n, \\
\psi_j^{**} &= \sum_{l=1}^{M-1} e^{-ik\mu_l^2/2}\ \widehat{\psi}_l^*\ \sin(\mu_l(x_j-a)), \qquad j = 1,2,\ldots,M-1, \\
\psi_j^{n+1} &= \exp\left\{-F\left(|\psi_j^{**}|^2, k/2\right) + i\left[-V(x_j)k/2 + G\left(|\psi_j^{**}|^2, k/2\right)\right]\right\}\ \psi_j^{**},
\end{aligned} \tag{2.13}$$

where $\widehat{U}_l$ are the sine-transform coefficients of a complex vector $U = (U_0, U_1, \ldots, U_M)$ with $U_0 = U_M = \mathbf{0}$ which are defined as

$$\mu_l = \frac{\pi l}{b-a}, \quad \widehat{U}_l = \frac{2}{M}\sum_{j=1}^{M-1} U_j\ \sin(\mu_l(x_j-a)),\ l = 1,2,\ldots,M-1, \tag{2.14}$$

where

$$\psi_j^0 = \psi(x_j,0) = \psi_0(x_j), \qquad j = 0,1,2,\ldots,M. \tag{2.15}$$

Note that the only time discretization error of the TSSP method is the splitting error, which is second-order in k if the integrals in (2.7) and (2.12) can be evaluated analytically.

2.2. Most frequently used damping terms. In this subsection we present explicit formulae for using the TSSP method when solving the NLS with those damping terms most frequently appearing in BEC and nonlinear optics.

Case I. *NLS with a linear damping term.* We choose $g(\rho) \equiv \delta$ with $\delta > 0$ in (1.5). In BEC, this damping term describes inelastic collisions of condensate particles with the background gas. From (2.7), we find

$$f(s) = \int \frac{1}{\delta s} ds = \frac{1}{\delta}\ln s \qquad \text{and} \qquad h(s,\tau) = e^{-2\delta\tau}\ s. \tag{2.16}$$

Substituting (2.16) into (2.9) and (2.12), we obtain

$$\rho(t) = e^{-2\delta(t-t_n)}\ |\psi(x,t_n)|^2, \quad t_n \le t \le t_{n+1}, \tag{2.17}$$

$$F(s,r) = \delta r, \tag{2.18}$$

$$G(s,r) = \frac{\beta s^\sigma}{2\delta\sigma}\left(1 - e^{-2\delta\sigma r}\right). \tag{2.19}$$

Substituting (2.18) and (2.19) into (2.13), we get the following second-order TSSP steps for the NLS with a linear damping term:

$$
\begin{aligned}
&\psi_j^* = \exp\left\{-k\delta/2 + i\left[-V(x_j)k/2 + \beta|\psi_j^n|^{2\sigma}\left(1-e^{-\delta\sigma k}\right)/(2\delta\sigma)\right]\right\}\ \psi_j^n,\\
&\psi_j^{**} = \sum_{l=1}^{M-1} e^{-ik\mu_l^2/2}\ \widehat{\psi}_l^*\ \sin(\mu_l(x_j-a)), \qquad j=1,2,\dots,M-1,\\
&\psi_j^{n+1} = \exp\left\{-k\delta/2 + i\left[-V(x_j)k/2 + \beta|\psi_j^{**}|^{2\sigma}\left(1-e^{-\delta\sigma k}\right)/(2\delta\sigma)\right]\right\}\ \psi_j^{**}.
\end{aligned}
\tag{2.20}
$$

Case II. *NLS with a damping term of the form* $g(\rho)=\delta\beta^q\rho^q$, *where* $\delta,\ q>0$ *in* (1.5). For $q=1$ ($q=2$), we obtain the damping term describing two (three) particle inelastic collisions in BEC. From (2.7) we get

$$
f(s) = \int \frac{1}{\delta\beta^q s^{q+1}} ds = -\frac{1}{q\delta\beta^q s^q} \qquad \text{and} \qquad h(s,\tau) = \frac{s}{\left(1+2q\delta\tau\beta^q s^q\right)^{1/q}}.
\tag{2.21}
$$

Substituting (2.21) into (2.9) and (2.12), we obtain

$$
\rho(t) = \frac{|\psi(x,t_n)|^2}{\left[1+2q\delta\beta^q(t-t_n)|\psi(x,t_n)|^{2q}\right]^{1/q}}, \quad t_n \le t \le t_{n+1},
\tag{2.22}
$$

$$
F(s,r) = \frac{1}{2q}\ln\left(1+2q\delta r\beta^q s^q\right),
\tag{2.23}
$$

$$
G(s,r) = \begin{cases} \dfrac{\beta^{1-q}}{2\delta q}\ln\left(1+2q\delta r\beta^q s^q\right), & q=\sigma,\\[2ex] \dfrac{\beta^{1-q}s^{\sigma-q}\left[-1+\left(1+2q\delta r\beta^q s^q\right)^{(q-\sigma)/q}\right]}{2\delta(q-\sigma)}, & \sigma\neq q. \end{cases}
\tag{2.24}
$$

Substituting (2.23) and (2.24) into (2.13), we get the following second-order TSSP method for the NLS:

(2.25)

$$
\psi_j^* = \begin{cases} \dfrac{\exp\left\{i\left[-V(x_j)k/2 + \beta^{1-q}\ln\left(1+\delta qk\beta^q|\psi_j^n|^{2q}\right)/(2\delta q)\right]\right\}}{\left(1+q\delta k\beta^q|\psi_j^n|^{2q}\right)^{1/2q}}\ \psi_j^n, & \sigma=q,\\[2ex] \dfrac{\exp\left\{i\left[-\frac{V(x_j)k}{2} + \frac{\beta^{1-q}|\psi_j^n|^{2\sigma-2q}}{2\delta(q-\sigma)}\left(-1+\left(1+\delta qk\beta^q|\psi_j^n|^{2q}\right)^{\frac{q-\sigma}{q}}\right)\right]\right\}}{\left(1+q\delta k\beta^q|\psi_j^n|^{2q}\right)^{1/2q}}\ \psi_j^n, & \sigma\neq q, \end{cases}
$$

$$
\psi_j^{**} = \sum_{l=1}^{M-1} e^{-ik\mu_l^2/2}\ \widehat{\psi}_l^*\ \sin(\mu_l(x_j-a)), \qquad j=1,2,\dots,M-1,
$$

$$
\psi_j^{n+1} = \begin{cases} \dfrac{\exp\left\{i\left[-V(x_j)k/2 + \beta^{1-q}\ln\left(1+\delta qk\beta^q|\psi_j^{**}|^{2q}\right)/(2\delta q)\right]\right\}}{\left(1+q\delta k\beta^q|\psi_j^{**}|^{2q}\right)^{1/2q}}\ \psi_j^{**}, & \sigma=q,\\[2ex] \dfrac{\exp\left\{i\left[-\frac{V(x_j)k}{2} + \frac{\beta^{1-q}|\psi_j^{**}|^{2\sigma-2q}}{2\delta(q-\sigma)}\left(-1+\left(1+\delta qk\beta^q|\psi_j^{**}|^{2q}\right)^{\frac{q-\sigma}{q}}\right)\right]\right\}}{\left(1+q\delta k\beta^q|\psi_j^{**}|^{2q}\right)^{1/2q}}\ \psi_j^{**}, & \sigma\neq q. \end{cases}
$$

Case III. *Focusing cubic NLS with a damping term that accounts for two-body and three-body losses in a BEC* [35]. We choose $\sigma=1$, $g(\rho)=\delta_1\beta\rho+\delta_2\beta^2\rho^2$ with

$\delta_1,\ \delta_2 > 0$, in (1.5). Using (2.7), we get

$$f(s) = \begin{cases} -\frac{1}{\delta_1\beta s} + \frac{\delta_2}{\delta_1^2}\ln\left(\delta_2\beta + \delta_1/s\right), & s > 0, \\ 0, & s = 0. \end{cases} \tag{2.26}$$

Substituting (2.7) into (2.12) and changing the variable of integration, we obtain

$$\begin{aligned} F(s,r) &= \int_0^r g\left(f^{-1}(f(s)-2\tau)\right)\, d\tau \overset{\tau=(f(s)-f(h))/2}{=} \int_s^{h(s,r)} -\frac{1}{2}g(h)f'(h)\, dh \\ &= \int_s^{h(s,r)} -\frac{1}{2h}\, dh = \begin{cases} -\frac{1}{2}\ln\left(h(s,r)/s\right), & s > 0, \\ 0, & s = 0, \end{cases} \end{aligned} \tag{2.27}$$

where $h(s,r)$ is the solution of

$$f(s) - f(h(s,r)) = 2r \qquad \text{for any } r > 0, \tag{2.28}$$

with f given in (2.26). Similarly we find

$$G(s,r) = \int_s^{h(s,r)} -\frac{\beta}{2g(h)}\, dh = \begin{cases} -\frac{1}{2\delta_1}\ln\frac{h(s,r)(\delta_1+\delta_2\beta s)}{s(\delta_1+\delta_2\beta h(s,r))}, & s > 0, \\ 0, & s = 0. \end{cases} \tag{2.29}$$

Substituting (2.27) and (2.29) into (2.13), we get the following second-order TSSP steps for the NLS with a combination of cubic and quintic damping terms:

(2.30)

$$\psi_j^* = \begin{cases} \dfrac{\sqrt{h(|\psi_j^n|^2,k/2)}}{|\psi_j^n|}\exp\left\{i\left[-\dfrac{V(x_j)k}{2} - \dfrac{1}{2\delta_1}\ln\dfrac{h(|\psi_j^n|^2,k/2)(\delta_1+\delta_2\beta|\psi_j^n|^2)}{|\psi_j^n|^2(\delta_1+\delta_2\beta h(|\psi_j^n|^2,k/2))}\right]\right\}\psi_j^n, & \psi_j^n \neq 0, \\ 0, & \psi_j^n = 0, \end{cases}$$

$$\psi_j^{**} = \sum_{l=1}^{M-1} e^{-ik\mu_l^2/2}\,\widehat{\psi}_l^*\,\sin(\mu_l(x_j-a)), \qquad j = 1,2,\ldots,M-1,$$

$$\psi_j^{n+1} = \begin{cases} \dfrac{\sqrt{h(|\psi_j^{**}|^2,k/2)}}{|\psi_j^{**}|}\exp\left\{i\left[-\dfrac{V(x_j)k}{2} - \dfrac{1}{2\delta_1}\ln\dfrac{h(|\psi_j^{**}|^2,k/2)(\delta_1+\delta_2\beta|\psi_j^{**}|^2)}{|\psi_j^{**}|^2(\delta_1+\delta_2\beta h(|\psi_j^{**}|^2,k/2))}\right]\right\}\psi_j^{**}, & \psi_j^{**} \neq 0, \\ 0, & \psi_j^{**} = 0. \end{cases}$$

Remark 2.1. As demonstrated in this subsection, the integrals in (2.7) and (2.12) can be evaluated *analytically* for the damping terms which most frequently appear in physical applications. If the integrals in (2.7) or (2.12) cannot be evaluated analytically or the inverse of f in (2.7) cannot be expressed explicitly, e.g., if $g(\rho)$ in (1.5) is not a polynomial, one can solve the following ODE numerically by either the second- or fourth-order Runge–Kutta method

$$\begin{aligned} &\frac{dh(t)}{dt} = -2g(h(t))\,h(t), \qquad 0 \le t \le k/2, \\ &h(0) = s, \end{aligned}$$

to get $h(s,k/2)$ for any given $s > 0$ and set $h(s,k/2) = 0$ for $s = 0$. By changing the variable of integration in (2.12) (see detail in (2.27) and (2.29)), the first integral in (2.12), i.e., $F(s,k/2)$, can be evaluated exactly (see detail in (2.27)), and the second

integral in (2.12), i.e., $G(s,k/2)=\int_s^{h(s,k/2)}-\frac{\beta h^{\sigma-1}}{2g(h)}\,dh$, can be evaluated numerically by using a numerical quadrature, e.g., the trapezoidal rule or Simpson's rule.

The TSSP scheme is explicit and is unconditionally stable as we will demonstrate in the next subsection. Another main advantage of the time-splitting method is its time transversal invariance, which also holds for the NLS and the DNLS themselves. If a constant α is added to the potential V, then the discrete wave functions $\psi_j^{\varepsilon,n+1}$ obtained from the TSSP method get multiplied by the phase factor $e^{-i\alpha(n+1)k}$, which leaves the discrete normalization unchanged. This property does not hold for finite difference schemes.

Remark 2.2. For the focusing cubic NLS with a quintic damping term describing three-body recombination loss and an additional feeding term for the BEC [25], we choose $\sigma=1$, $g(\rho)=-\delta_1+\delta_2\beta^2\rho^2$ with $\delta_1,\delta_2>0$ in (1.5). The idea of constructing the TSSP method is also applicable to this case, although we could not prove that it is unconditionally stable due to the feeding term. Inserting the above feeding term into (2.7), we get

$$f(s)=\begin{cases}\frac{1}{2\delta_1}\ln\left|\delta_2\beta^2-\delta_1/s^2\right|, & s>0,\\ 0, & s=0.\end{cases}\tag{2.31}$$

Inserting (2.31) into (2.9), we find

$$h(s,\tau)=\frac{s\sqrt{\delta_1}}{\sqrt{\delta_1 e^{-4\tau\delta_1}+(1-e^{-4\tau\delta_1})\delta_2\beta^2 s^2}},\tag{2.32}$$

and substituting (2.32) into (2.9) and (2.12), we obtain

$$\rho(t)=\frac{|\psi(x,t_n)|^2\sqrt{\delta_1}}{\sqrt{\delta_1 e^{-4\tau\delta_1}+(1-e^{-4\tau\delta_1})\delta_2\beta^2|\psi(x,t_n)|^4}},\ t_n\le t\le t_{n+1},\tag{2.33}$$

$$F(s,r)=-\delta_1 r+\frac{1}{4}\ln\left[1+\delta_2\beta^2 s^2(e^{4\delta_1 r}-1)/\delta_1\right],\tag{2.34}$$

$$G(s,r)=\frac{1}{2\sqrt{\delta_1\delta_2}}\ln\frac{\beta s\sqrt{\delta_2}e^{2r\delta_1}+\sqrt{\delta_1+\delta_2\beta^2 s^2\left(e^{4r\delta_1}-1\right)}}{\sqrt{\delta_1}+\beta s\sqrt{\delta_2}}.\tag{2.35}$$

Inserting (2.34) and (2.35) into (2.13), we get the following second-order TSSP steps for the NLS with a quintic damping term and a feeding term:

(2.36)

$$\psi_j^*=\frac{e^{k\delta_1/2}\exp\left[i\left(-\frac{V(x_j)k}{2}+\frac{1}{2\sqrt{\delta_1\delta_2}}\ln\frac{\beta|\psi_j^n|^2\sqrt{\delta_2}e^{k\delta_1}+\sqrt{\delta_1+\delta_2\beta^2|\psi_j^n|^4\left(e^{2k\delta_1}-1\right)}}{\sqrt{\delta_1}+\beta|\psi_j^n|^2\sqrt{\delta_2}}\right)\right]}{\left[1+\delta_2\beta^2|\psi_j^n|^4(e^{2k\delta_1}-1)/\delta_1\right]^{1/4}}\,\psi_j^n,$$

$$\psi_j^{**}=\sum_{l=1}^{M-1}e^{-ik\mu_l^2/2}\,\widehat{\psi}_l^*\,\sin(\mu_l(x_j-a)),\qquad j=1,2,\dots,M-1,$$

$$\psi_j^{n+1}=\frac{e^{k\delta_1/2}\exp\left[i\left(-\frac{V(x_j)k}{2}+\frac{1}{2\sqrt{\delta_1\delta_2}}\ln\frac{\beta|\psi_j^{**}|^2\sqrt{\delta_2}e^{k\delta_1}+\sqrt{\delta_1+\delta_2\beta^2|\psi_j^{**}|^4\left(e^{2k\delta_1}-1\right)}}{\sqrt{\delta_1}+\beta|\psi_j^{**}|^2\sqrt{\delta_2}}\right)\right]}{\left[1+\delta_2\beta^2|\psi_j^{**}|^4(e^{2k\delta_1}-1)/\delta_1\right]^{1/4}}\,\psi_j^{**}.$$

Remark 2.3. The TSSP scheme (2.13) can easily be extended for solving the complex Ginzburg–Landau (CGL) equation [15, 28]

$$i\,\psi_t=-\left(1-i\,\varepsilon\right)\Delta\psi-|\psi|^2\psi-i\left(\delta_2|\psi|^2-\delta_1\right)\psi,\tag{2.37}$$

where ε, δ_1, and δ_2 are positive constants. The idea of constructing the TSSP method for the DNLS is also applicable to the CGL equation provided that we solve

$$i\,\psi_t = -\,(1 - i\,\varepsilon)\,\Delta\psi \tag{2.38}$$

in the first step instead of (2.3). Inserting $\sigma = 1$, $\beta = 1$, and $g(\rho) = \delta_2\rho - \delta_1$ with δ_1, $\delta_2 > 0$ into (1.5) and using (2.7), we get

$$f(s) = \begin{cases} \frac{1}{\delta_1} \ln\left|\delta_2 - \delta_1/s\right|, & s > 0, \\ 0, & s = 0. \end{cases} \tag{2.39}$$

Inserting (2.39) into (2.7), we find

$$h(s,\tau) = \frac{s\delta_1}{s\delta_2\,(1 - e^{-2\tau\delta_1}) + \delta_1 e^{-2\tau\delta_1}}, \tag{2.40}$$

and substituting (2.40) into (2.9) and (2.12), we obtain

$$\rho(t) = \frac{\delta_1\,|\psi(x,t_n)|^2}{\delta_2\,|\psi(x,t_n)|^2\,(1 - e^{-2\tau\delta_1}) + \delta_1 e^{-2\tau\delta_1}},\ t_n \le t \le t_{n+1}, \tag{2.41}$$

$$F(s,r) = -\frac{1}{2} \ln \frac{\delta_1}{s\delta_2 + (\delta_1 - s\delta_2)\,e^{-2r\delta_1}}, \tag{2.42}$$

$$G(s,r) = \frac{1}{2\delta_2} \ln \frac{\delta_1 - s\delta_2 + s\delta_2 e^{2r\delta_1}}{\delta_1}. \tag{2.43}$$

Inserting (2.42) and (2.43) into (2.13), we get the following second-order TSSP steps for the CGL equation (2.37):

(2.44)

$$\psi_j^* = \sqrt{\frac{\delta_1}{\delta_2|\psi_j^n|^2 + \left(\delta_1 - \delta_2|\psi_j^n|^2\right) e^{-k\delta_1}}}\, \exp\left[\frac{i}{2\delta_2} \ln \frac{\delta_1 - \delta_2|\psi_j^n|^2 + \delta_2|\psi_j^n|^2 e^{k\delta_1}}{\delta_1}\right]\ \psi_j^n,$$

$$\psi_j^{**} = \sum_{l=1}^{M-1} e^{-(\varepsilon+i)k\mu_l^2}\ \widehat{\psi}_l^*\ \sin(\mu_l(x_j - a)), \qquad j = 1, 2, \ldots, M-1,$$

$$\psi_j^{n+1} = \sqrt{\frac{\delta_1}{\delta_2|\psi_j^{**}|^2 + \left(\delta_1 - \delta_2|\psi_j^{**}|^2\right) e^{-k\delta_1}}}\, \exp\left[\frac{i}{2\delta_2} \ln \frac{\delta_1 - \delta_2|\psi_j^{**}|^2 + \delta_2|\psi_j^{**}|^2 e^{k\delta_1}}{\delta_1}\right]\ \psi_j^{**}.$$

Remark 2.4. If the homogeneous periodic boundary conditions in (2.2) are replaced by the periodic boundary conditions

$$\psi(a,t) = \psi(b,t), \qquad \psi_x(a,t) = \psi_x(b,t), \qquad t \ge 0, \tag{2.45}$$

the TSSP scheme (2.13) still works provided that one replaces the sine-series in (2.13) by a Fourier series [4, 5, 7].

2.3. Stability and decay rate. Let $U = (U_0, U_1, \ldots, U_M)^T$ with $U_0 = U_M = \mathbf{0}$ and $\|\cdot\|_{l^2}$ be the usual discrete l^2-norm on the interval (a,b), i.e.,

$$\|U\|_{l^2} = \sqrt{\frac{b-a}{M} \sum_{j=1}^{M-1} |U_j|^2}. \tag{2.46}$$

For the *stability* of the TSSP approximations (2.13), we have the following lemma, which shows that the total normalization does not increase.

LEMMA 2.1. *The TSSP schemes* (2.13) *are unconditionally stable if* $g(s) \geq 0$ *for* $s \geq 0$. *In fact, for every mesh size* $h > 0$ *and time step* $k > 0$,

$$\|\psi^{n+1}\|_{l^2} \leq \|\psi^n\|_{l^2} \leq \|\psi^0\|_{l^2} = \|\psi_0\|_{l^2}, \qquad n = 0, 1, 2, \ldots. \tag{2.47}$$

Furthermore, when a linear damping term is used in (1.5), *i.e., when we choose* $g(\rho) \equiv \delta$ *with* $\delta > 0$, *the decay rate of the normalization satisfies*

$$\|\psi^n\|_{l^2} = e^{-2\delta t_n}\|\psi^0\|_{l^2} = e^{-2\delta t_n}\|\psi_0\|_{l^2}, \qquad n = 1, 2, \ldots. \tag{2.48}$$

In fact, (2.48) *is a discretized version of the decay rate of the normalization* $N(t)$ *in* (1.8).

Proof. We combine (2.13), (2.14), and (2.46) and note that $F(s, \tau) \geq 0$ for $s \geq 0$ and $\tau \geq 0$ to obtain

$$\begin{aligned}
\frac{1}{b-a}\|\psi^{n+1}\|_{l^2}^2 &= \frac{1}{M}\sum_{j=1}^{M-1}\left|\psi_j^{n+1}\right|^2 \\
&= \frac{1}{M}\sum_{j=1}^{M-1}\exp\left[-2F\left(|\psi_j^{**}|^2, k/2\right)\right]\left|\psi_j^{**}\right|^2 \leq \frac{1}{M}\sum_{j=1}^{M-1}\left|\psi_j^{**}\right|^2 \\
&= \frac{1}{M}\sum_{j=1}^{M-1}\left|\sum_{l=1}^{M-1} e^{-ik\mu_l^2/2}\,\widehat{\psi}_l^*\,\sin(\mu_l(x_j-a))\right|^2 = \frac{1}{2}\sum_{l=1}^{M-1}\left|e^{-ik\mu_l^2/2}\,\hat{\psi}_l^*\right|^2 = \frac{1}{2}\sum_{l=1}^{M-1}\left|\hat{\psi}_l^*\right|^2 \\
&= \frac{1}{2}\sum_{l=1}^{M-1}\left|\frac{2}{M}\sum_{j=1}^{M-1}\psi_j^*\,\sin(\mu_l(x_j-a))\right|^2 = \frac{1}{M}\sum_{j=1}^{M-1}\left|\psi_j^*\right|^2 \\
&= \frac{1}{M}\sum_{j=1}^{M-1}\exp\left[-2F\left(|\psi_j^n|^2, k/2\right)\right]\left|\psi_j^n\right|^2 \leq \frac{1}{M}\sum_{j=1}^{M-1}\left|\psi_j^n\right|^2 \\
&= \frac{1}{b-a}\|\psi^n\|_{l^2}^2.
\end{aligned} \tag{2.49}$$

Here, we used the identity

$$\sum_{j=1}^{M-1}\sin\left(\frac{\pi r\, j}{M}\right)\,\sin\left(\frac{\pi s\, j}{M}\right) = \begin{cases} 0, & r-s \neq 2mM, \\ M/2, & r-s = 2mM, r \neq 2nM, \end{cases} \qquad m, n \text{ integer}. \tag{2.50}$$

When a linear damping term is added to the NLS (1.5), the equality (2.48) follows from the above proof, (2.18), and

$$\sum_{j=1}^{M-1}\exp\left[-2F\left(|\psi_j^n|^2, k/2\right)\right]\left|\psi_j^n\right|^2 = \sum_{j=1}^{M-1} e^{-\delta k}\left|\psi_j^n\right|^2 = e^{-\delta k}\sum_{j=1}^{M-1}\left|\psi_j^n\right|^2.$$

3. Numerical examples. In this section, we present numerical tests of the TSSP scheme (2.13) for solving a focusing cubic NLS appearing in nonlinear optics [16, 36] and for the GPE in BEC [7] in two dimensions with a linear, a cubic, or a quintic

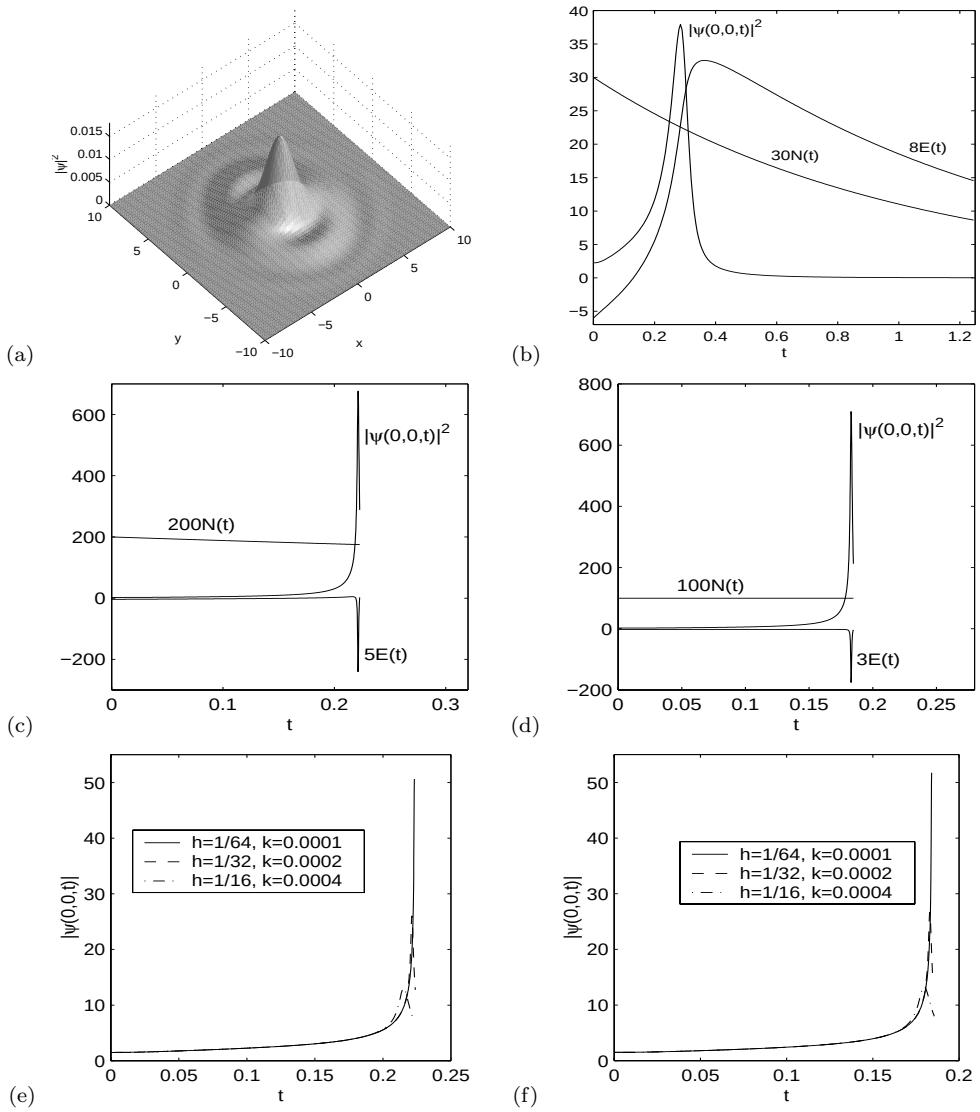

FIG. 1. *Numerical results in Example* 1*, case* I. (a) *Surface plot of the density* $|\psi|^2$ *at time* $t = 1.25$ *with* $\delta = 0.5$. *Normalization, energy, and central density* $|\psi(0,0,t)|^2$ *as functions of time:* (b) *with* $\delta = 0.5$, (c) $\delta = 0.3$, (d) $\delta = 0$ *(no damping). Blowup study:* (e) $\delta = 0.3$, (f) $\delta = 0$ *(no damping).*

damping term. In our computations, the initial condition (1.2) is always chosen such that $|\psi_0(\mathbf{x})|$ decays to zero sufficiently fast as $|\mathbf{x}| \to \infty$. We choose an appropriately large rectangle $[a, b] \times [c, d]$ in two dimensions to prevent the homogeneous periodic boundary condition (2.2) from introducing a significant (aliasing) error relative to the whole space problem. To quantify the numerical results of the GPE for a BEC, we define the condensate widths along the x, y, and z axes by

$$\sigma_\alpha^2 = \langle \alpha^2 \rangle = \frac{1}{N(t)} \int_{\mathbb{R}^d} \alpha^2 |\psi(\mathbf{x}, t)|^2 \, d\mathbf{x}, \qquad \text{with} \quad \alpha = x, \ y, \ \text{or} \ z.$$

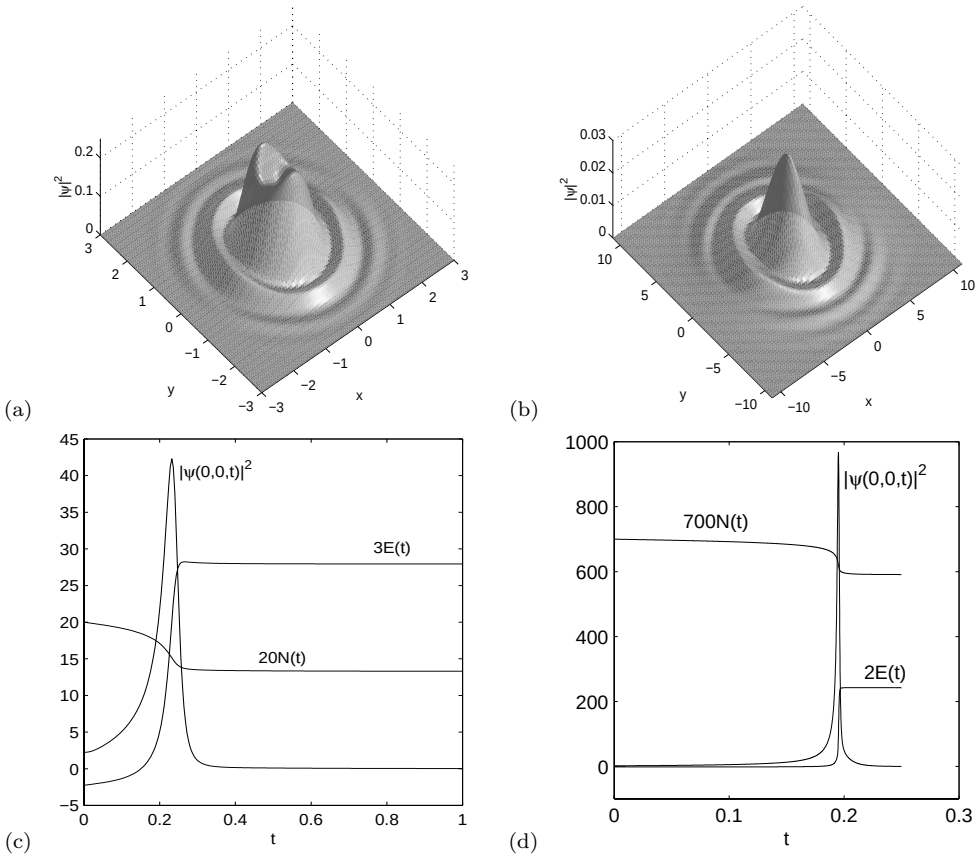

FIG. 2. *Numerical results in Example* 1*, case* II. *Surface plot of the density* $|\psi|^2$ *with* $\delta = 0.02$*:* (a) *At time* $t = 0.4$*,* (b) $t = 1.0$*. Normalization, energy, and central density* $|\psi(0,0,t)|^2$ *as functions of time:* (c) *with* $\delta = 0.02$*,* (d) $\delta = 0.005$ *(with* $h = 1/128$*,* $k = 0.00002$*).*

Example 1. *Solution of the two-dimensional damped focusing cubic NLS.* We choose $d = 2$, $\sigma = 1$, and $V(x, y) \equiv 0$ in (1.5) and present computations for three different damping terms ($\delta > 0$):

I. A linear damping term; i.e., we choose $g(\rho) \equiv \delta$.

II. A cubic damping term; i.e., we choose $g(\rho) \equiv \delta\beta\rho$.

III. A quintic damping term; i.e., we choose $g(\rho) \equiv \delta\beta^2\rho^2$.

The initial condition (1.6) is taken to be

$$\psi(x, y, 0) = \psi_0(x, y) = \frac{\gamma_y^{1/4}}{\sqrt{\pi\varepsilon}}\, e^{-(x^2+\gamma_y y^2)/2\varepsilon}, \qquad (x, y) \in \mathbb{R}^2. \tag{3.1}$$

We assume $\gamma_y = 2$, $\varepsilon = 0.2$, and $\beta = 8$ in (1.5) such that $E(0) = -0.751582 < 0$ in (1.4). We solve the NLS on the square $[-16, 16]^2$; i.e., $a = c = -16$ and $b = d = 16$ with mesh size $h = \frac{1}{32}$, time step $k = 0.0002$, and homogeneous periodic boundary conditions along the boundary of the square. We compare the effect of changing the damping parameter δ in the three different cases I, II, and III.

Figure 1 shows the surface plot of the density $|\psi(x, y, t)|^2$ at time $t = 1.25$ with $\delta = 0.5$; plots of the normalization, energy, and central density $|\psi(0, 0, t)|^2$ are shown

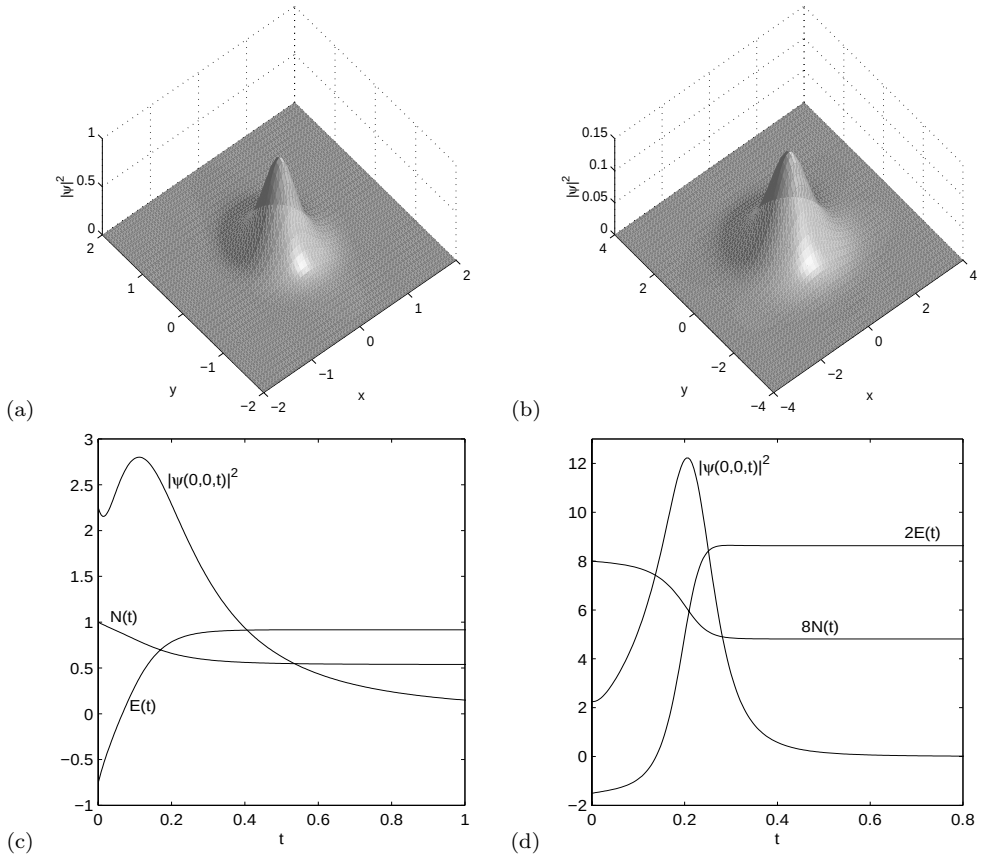

FIG. 3. *Numerical results in Example* 1, *case* III. *Surface plot of the density* $|\psi|^2$ *with* $\delta = 0.01$*:* (a) *At time* $t = 0.4$, (b) $t = 1.0$. *Normalization, energy, and central density* $|\psi(0,0,t)|^2$ *as functions of time:* (c) *with* $\delta = 0.01$, (d) $\delta = 0.001$.

as functions of time with $\delta = 0.5,\ 0.3$, and $\delta = 0$ (no damping) for case I. Figure 2 shows similar results for case II and Figure 3 for case III. Furthermore, Figure 4 shows contour plots of the density $|\psi|^2$ at different times for case III with $\delta = 0.01$.

In the numerical computations, a blowup is detected either from the plot of the central density $|\psi(0,0,t)|^2$, which at the blowup shows a very sharp spike with a peak value that increases when the mesh size h decreases, or from the plot of the energy $E(t)$, which has a very sharp spike with negative values at the blowup. In fact, the TSSP method (2.13) aims to capture the solution of the DNLS without blowup, i.e., physical relevant solution. If one wants to capture the blowup rate of the NLS, we refer to [27, 31].

From the numerical results we find the following conditions for arresting a blowup of the wave function with initial energy $E(0) < 0$. (1) For linear damping, the blowup is arrested if the damping parameter is bigger than a certain threshold value which we find to be $\delta_{\rm th} \approx 0.461$ by numerical experiments. As shown in Figure 1(b), blowup is arrested for $\delta = 0.5 > \delta_{\rm th}$, while the wave function blows up for $\delta < \delta_{\rm th}$, as can be seen from Figure 1(c),(d), where we have chosen $\delta = 0.3 < \delta_{\rm th}$ and $\delta = 0 < \delta_{\rm th}$, respectively. The time at which the blowup of the wave function happens, however, increases with increasing δ (cf. Figure 1(c)(d)). (2) For a cubic damping term with

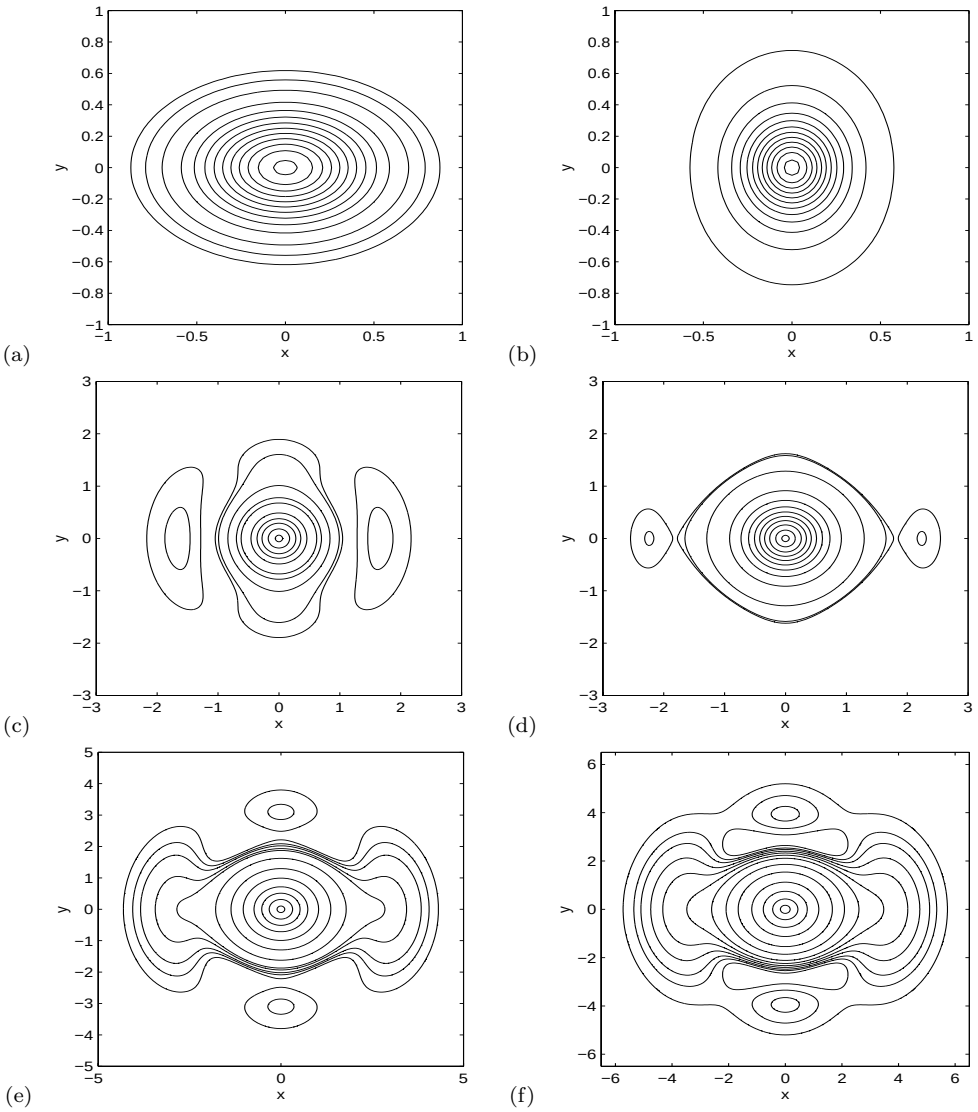

FIG. 4. *Contour plots of the density* $|\psi|^2$ *at different times in Example* 1*, case* III*, with* $\delta = 0.01$. (a) $t = 0$, (b) $t = 0.2$, (c) $t = 0.4$, (d) $t = 0.6$, (e) $t = 0.8$, (f) $t = 1$.

$\delta > 0$, the blowup of the wave function is always arrested (cf. Figure 2). (3) The above observation (2) also holds for a quintic damping term (cf. Figure 3).

For linear damping, we also test the dependence of the threshold value of the damping parameter $\delta_{\rm th}$ on β and the initial data. First we take $\gamma_y = 2$ and $\varepsilon = 0.2$ in (3.1). Table 1 shows the threshold values $\delta_{\rm th}$ for different β in (1.5), and $E(0)$ represents the initial energy. Then we choose $\beta = 16$ in (1.5) and $\gamma_y = 2$ in (3.1). Table 2 displays the threshold values $\delta_{\rm th}$ for different values of ε in (3.1).

From Table 1, we find by a least square fitting

$$\delta_{\rm th} = -0.6930E(0) \qquad \text{or} \qquad \delta_{\rm th} = 0.3872\beta - 2.4627.$$

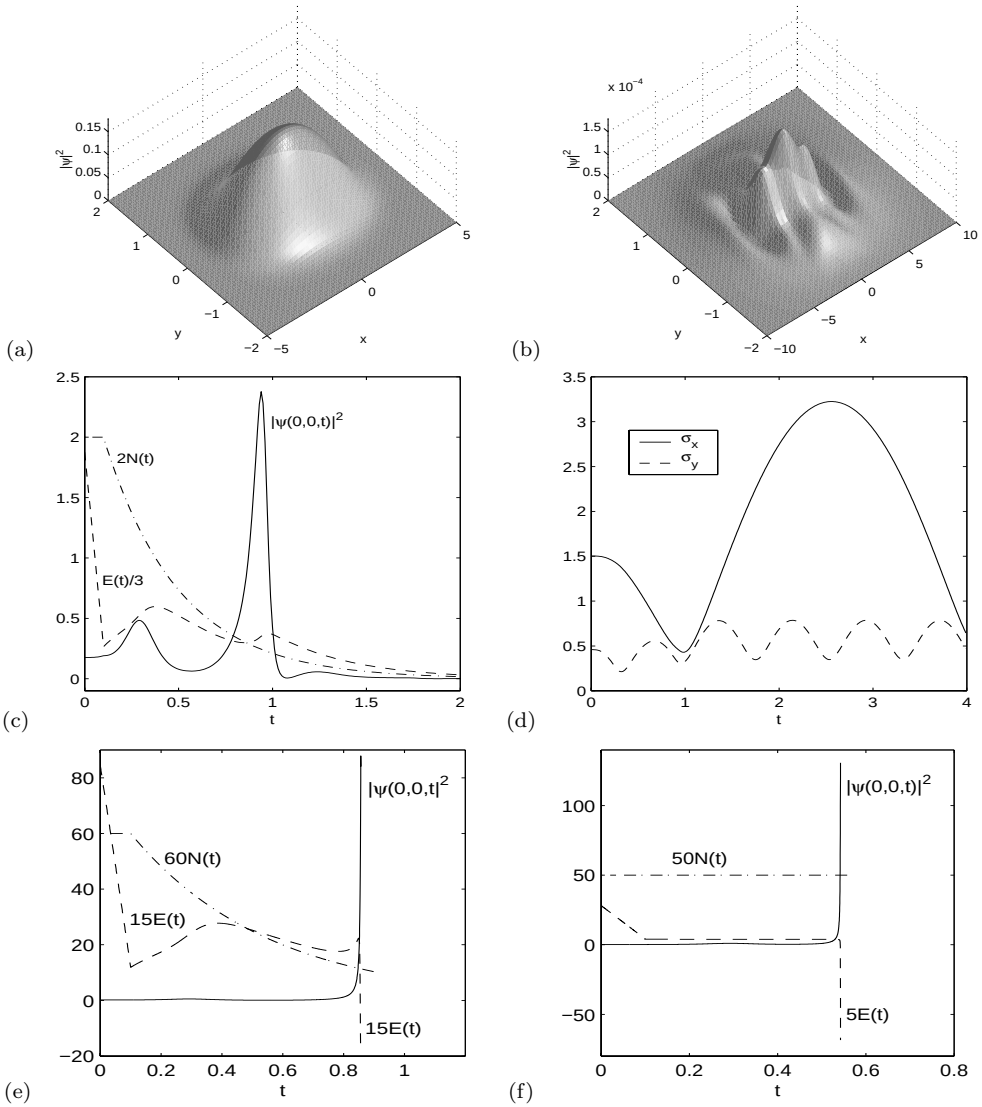

FIG. 5. *Numerical results in Example* 2, *case* I. *Surface plot of the density* $|\psi|^2$ *with* $\delta = 1.25$*:* (a) *At time* $t = 0$ *(ground-state solution),* (b) $t = 2.8$. *Normalization, energy, and central density* $|\psi(0,0,t)|^2$ *as functions of time:* (c) *with* $\delta = 1.25$, (e) $\delta = 1.1$, (f) $\delta = 0$ *(no damping).* (d) *Condensate widths with* $\delta = 1.25$.

TABLE 1
Dependence of $\delta_{\rm th}$ *on* β *for* $\gamma_y = 2$ *and* $\varepsilon = 0.2$ *in* (3.1).

	$\beta = 8$	$\beta = 16$	$\beta = 32$	$\beta = 64$	$\beta = 128$
$E(0)$	-0.7516	-5.253	-14.256	-32.263	-68.275
$\delta_{\rm th}$	0.461	3.655	10.35	22.15	40.05

TABLE 2
Dependence of $\delta_{\rm th}$ *on* ε *in* (3.1) *for* $\beta = 16$ *in* (1.5) *and* $\gamma_y = 2$ *in* (3.1).

	$\varepsilon = 0.8$	$\varepsilon = 0.4$	$\varepsilon = 0.2$	$\varepsilon = 0.1$	$\varepsilon = 0.05$
$E(0)$	-1.3133	-2.6266	-5.2532	-10.506	-21.013
$\delta_{\rm th}$	0.895	1.845	3.655	7.25	14.55

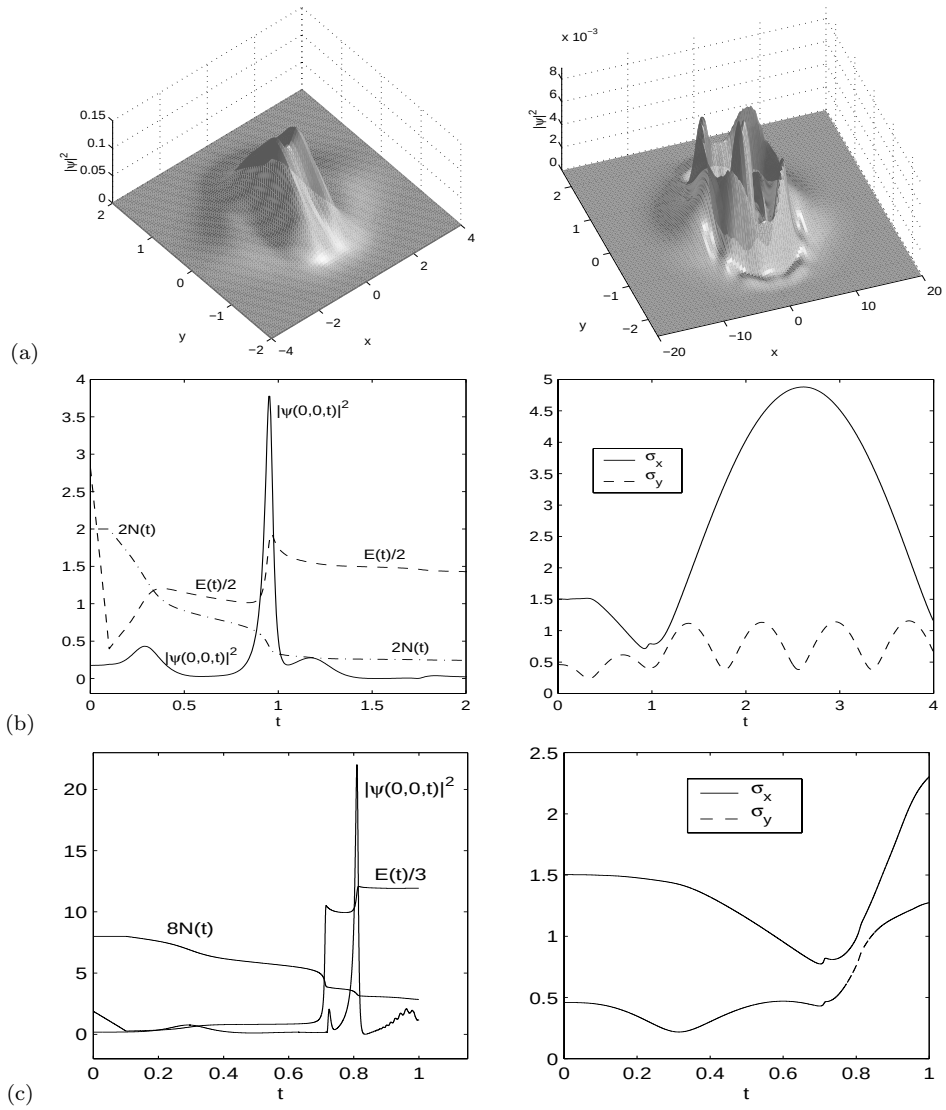

FIG. 6. *Numerical results in Example* 2*, case* II. (a) *Surface plot of the density* $|\psi|^2$ *with* $\delta = 0.15$*: At time* $t = 0.8$ *(left column) and* $t = 2.4$ *(right column). Normalization, energy, and central density* $|\psi(0,0,t)|^2$ *(left column) and condensate widths (right column) as functions of time:* (b) *With* $\delta = 0.15$*;* (c) $\delta = 0.04$ *(under* $h = 1/128, k = 0.00002$ *for* (c)*).*

Similarly, from Table 2, we obtain

$$\delta_{\text{th}} = -0.6922E(0).$$

Based on this observation, we conclude that the threshold value of the linear damping parameter δ_{th} depends linearly on the initial energy $E(0)$.

Example 2. *Solution of the two-dimensional damped GPE with focusing nonlinearity.* We choose $d = 2$, $\sigma = 1$, and $V(x,y) = \frac{1}{2}(\gamma_x^2 x^2 + \gamma_y^2 y^2)$ to be a harmonic oscillator potential with $\gamma_x, \gamma_y > 0$ in (1.5). Again, we present computations for the same three different damping terms in (1.5) that we studied in Example 1.

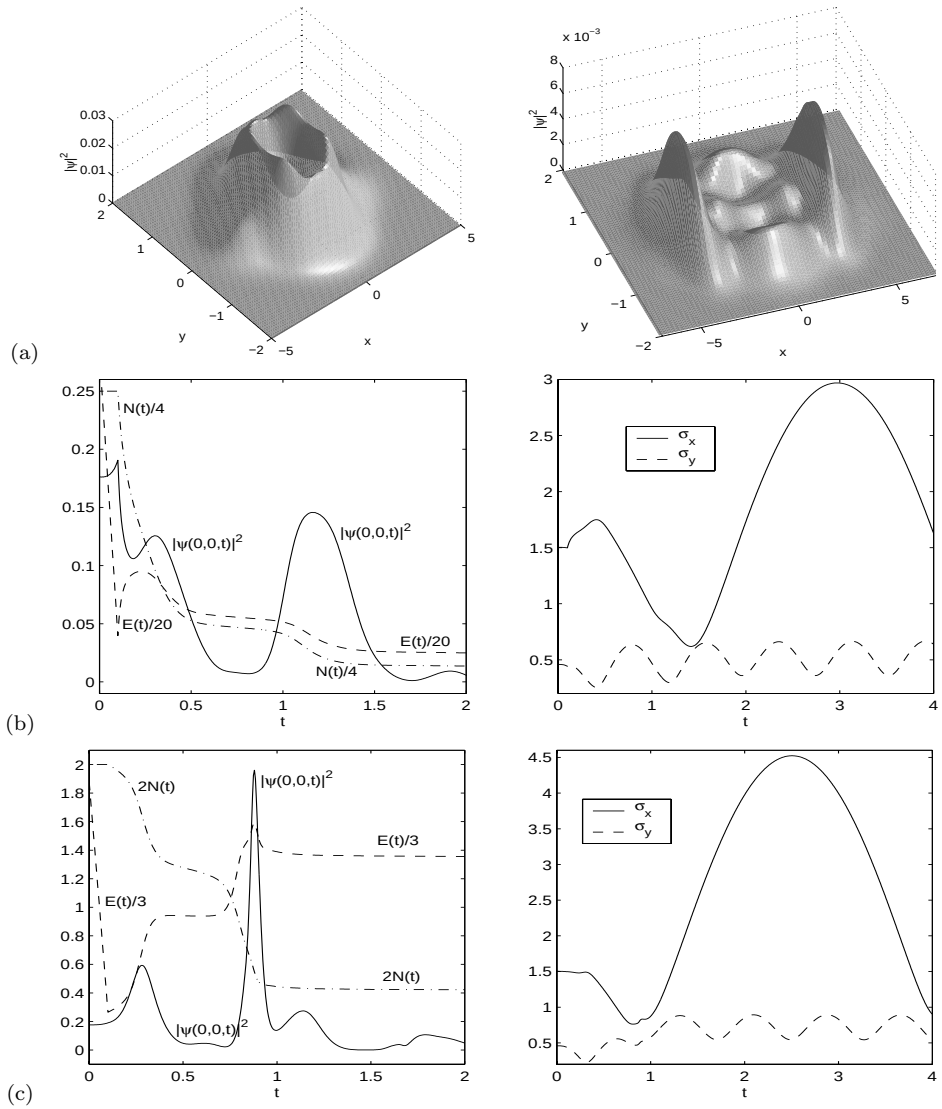

FIG. 7. *Numerical results in Example* 2, *case* III. (a) *Surface plot of the density* $|\psi|^2$ *with* $\delta = 0.15$*: At time* $t = 0.8$ *(left column) and* $t = 3.2$ *(right column). Normalization, energy, and central density* $|\psi(0,0,t)|^2$ *(left column) and condensate widths (right column) as functions of time:* (b) *With* $\delta = 0.15$*;* (c) $\delta = 0.005$.

We take $\gamma_x = 1$ and $\gamma_y = 4$. The initial condition (1.6) is assumed to be the ground-state solution of (1.5) with $g(\rho) \equiv 0$ (i.e., undamped case) and $\beta = -40$ [6]. The cubic nonlinearity is ramped linearly from $\beta = -40$ (defocusing) to $\beta = 50$ (focusing) during the time interval $[0, 0.1]$ and afterward kept constant. The absorption parameter was set to $\delta = 0$ during the time interval $[0, 0.1]$ and increased to a positive value $\delta > 0$ afterward.

We solve the GPE on the rectangle $[-24, 24] \times [-6, 6]$, i.e., for $a = -24$, $b = 24$, $c = -6$, and $d = 6$ with mesh size $h_x = \frac{3}{64}$, $h_y = \frac{3}{128}$, time step $k = 0.0005$, and homogeneous periodic boundary conditions along the boundary of the rectangle.

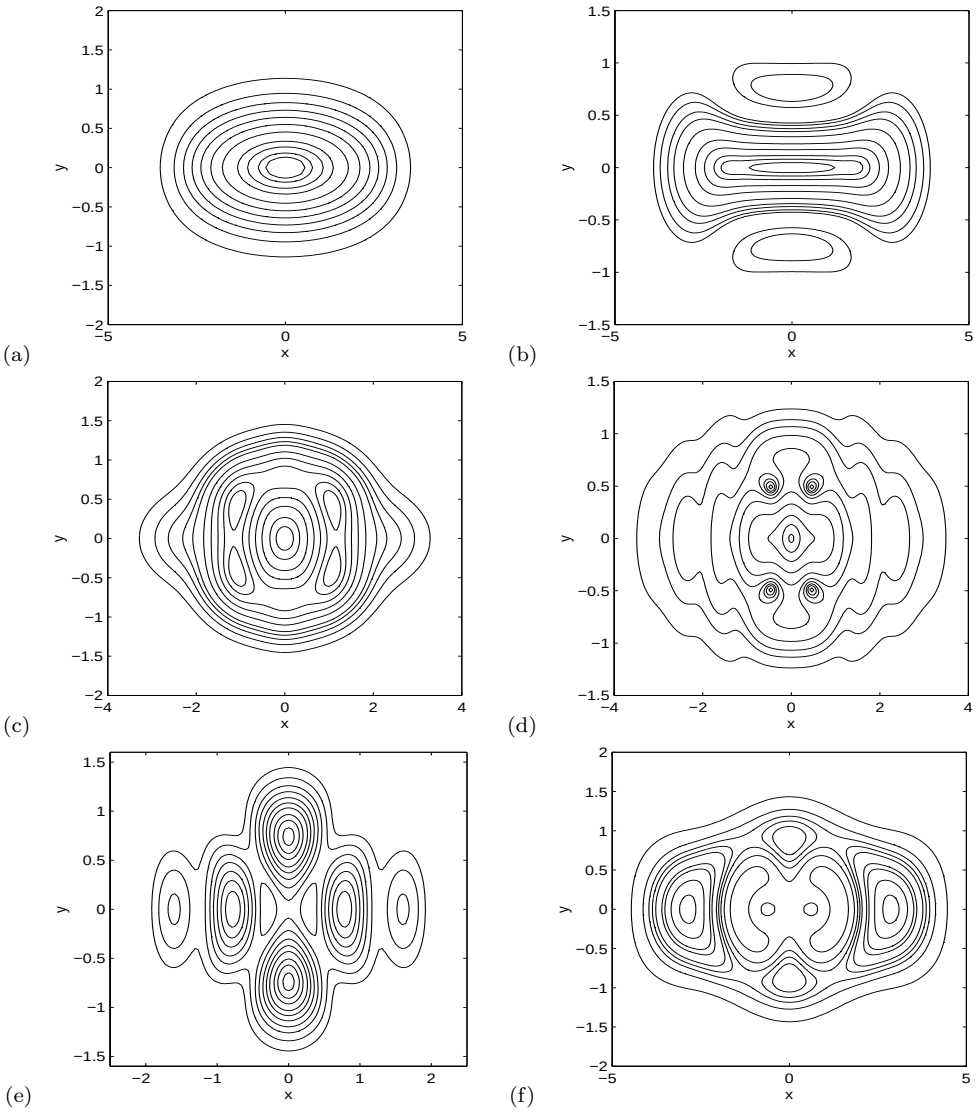

FIG. 8. *Contour plots of the density* $|\psi|^2$ *at different times in Example* 2, *case* III, *with* $\delta = 0.15$. (a) $t = 0$, (b) $t = 0.4$, (c) $t = 0.8$, (d) $t = 1.2$, (e) $t = 1.6$, (f) $t = 2.4$.

Again, we compare the effect of changing the damping parameter δ in the three different cases I, II, and III.

Figure 5 shows a surface plot of the density $|\psi(x, y, t)|^2$ at times $t = 0$ (ground-state solution) and $t = 2.8$ with $\delta = 1.25$; normalization, energy, and central density $|\psi(0, 0, t)|^2$ are shown as functions of time with $\delta = 1.25$, 1.1, and 0 (no damping) for case I. Figure 6 shows similar results for case II and Figure 7 for case III. Furthermore, Figure 8 shows contour plots of the density $|\psi|^2$ at different times for case III with $\delta = 0.15$.

From our numerical results we find that the observations (1)–(3) made for Example 1 are still valid with the additional trapping potential. However, the value of δ_{th} depends on β (or initial energy $E(0)$), and we find $\delta_{\text{th}} \approx 1.185$ for linear damping

(cf. Figure 5).

3.1. Discussion. In this subsection, we discuss our numerical results in terms of physical properties of a BEC described by the GPE. We concentrate on those cases where a collapse of the wave function is arrested since this collapse leads to unphysical processes like the negative peaks in the energy $E(t)$ shown in Figures 1(c), (d) and 5(e), (f).

The general form of the time evolution in Example 1 is similar for all three cases. Initially the cloud of atoms contracts due to the attractive interaction between the particles. This contraction is accompanied by an increase in the energy due to particle loss which is most efficient in regions of high particle density. These regions are characterized by a negative local energy density leading to an increase in energy for each particle lost there. After the central particle density has reached a maximum, the cloud starts to expand due to the kinetic energy gained by the particles during the contraction. Particles are emitted from the cloud in burst-like pulses which can be seen in Figures 4 and 8. Such bursts have also been seen in BEC experiments [12]. The main differences between the three cases are the behavior of the energy and the number of particles as a function of time. In case I, where we assumed a linear damping term, the loss rate of particles from the condensate is independent of the shape of the condensate wave function. The energy decrease during the condensate expansion is determined by the loss of particles (cf. Figure 1(b)). In the cases of cubic and quintic damping, the loss term has a significant effect only on the time evolution of the condensate during the contraction. When the condensate expands, the density of particles is so low that the loss terms have only a very small effect and the energy $E(t)$ and the number of particles $N(t)$ remain almost constant (see Figures 2(c) and 3(c), (d)).

In Example 2, we add an additional trap potential which confines the BEC, and we assume a realistic scenario (described above) to prepare the condensate in the trap (cf. the experiments by Donley et al. [12]). We find that the initial process of turning on the attractive interactions between the particles leads to oscillations in the widths of the condensate [7] as can be seen from Figures 5, 6, and 7. However, neither the additional trap potential nor these oscillations significantly alter the behavior of the system compared to Example 1, when the condensate is strongly contracted. Before and after this contraction, some differences can be seen. By looking at Figures 5 and 6 we find that the first minimum in σ_y due to the oscillations of the condensate causes an increase in the central density and in the energy. For cubic and quintic damping, this is accompanied by an increased particle loss. However, an arrested collapse of the wave function happens only when both σ_x and σ_y attain a minimum value due to the attractive interactions (cf. Figures 5(d) and 6(b)). We also note that the frequency of the oscillations after an arrested collapse has happened is not significantly influenced by the damping terms. The amplitude of these oscillations is, however, strongly dependent on δ and decreases with increasing δ. Finally, we want to mention that a series of contractions and expansions of the condensate is possible. In Figure 7(b), we find three contractions of the condensate where only the first one reaches a sufficiently high particle density to lead to an increase in energy while the next two contractions show a rather smooth decrease in energy and particle number. For a smaller quintic damping term, we obtain two contractions of the condensate which increase the energy (see Figure 7(c)).

4. Conclusions. We extended the explicit unconditionally stable second-order TSSP method for solving damped focusing NLSs. We showed that this method is

time transversal invariant and preserves the exact decay rate of the normalization for a linear damping of the NLS. Extensive numerical tests were presented for the cubic focusing NLS in two dimensions with linear, cubic, and quintic damping terms. Our numerical results show that quintic and cubic damping always arrest blowup, whereas linear damping can arrest blowup only when the damping parameter δ is bigger than a certain threshold value $\delta_{\rm th}$. We will apply this novel method to solve the three-dimensional GPE with a quintic damping term and will compare the numerical results with the experimental dynamics [12] of collapsing and exploding BECs [8].

Acknowledgment. The authors acknowledge the hospitality of the International Erwin Schrödinger Institute in Vienna, where this work was initiated.

REFERENCES

[1] S. K. Adhikari, *Mean-field description for collapsing and exploding Bose-Einstein condensates*, Phys. Rev. A, 66 (2002), pp. 3611–3615.

[2] M. H. Anderson, J. R. Ensher, M. R. Matthews, C. E. Wieman, and E. A. Cornell, *Observation of Bose-Einstein condensation in a dilute atomic vapor*, Science, 269 (1995), pp. 198–201.

[3] J. R. Anglin and W. Ketterle, *Bose-Einstein condensation of atomic gases*, Nature, 416 (2002), pp. 211–218.

[4] W. Bao, S. Jin, and P. A. Markowich, *On time-splitting spectral approximations for the Schrödinger equation in the semiclassical regime*, J. Comput. Phys., 175 (2002), pp. 487–524.

[5] W. Bao, S. Jin, and P. A. Markowich, *Numerical study of time-splitting spectral discretizations of nonlinear Schrödinger equations in the semiclassical regimes*, SIAM J. Sci. Comput., 25 (2003), pp. 27–64.

[6] W. Bao and W. Tang, *Ground state solution of trapped interacting Bose-Einstein condensate by minimizing a functional*, J. Comput. Phys., 187 (2003), pp. 230–254.

[7] W. Bao, D. Jaksch, and P. A. Markowich, *Numerical solution of the Gross-Pitaevskii equation for Bose-Einstein condensation*, J. Comput. Phys., 187 (2003), pp. 318–342.

[8] W. Bao, D. Jaksch, and P. A. Markowich, *Three Dimensional Simulation of Jet Formation in Collapsing Condensates*, preprint, 2003. Available online from http://arXiv.org/abs/cond-mat/0307344.

[9] R. Ciegis and V. Pakalnyte, *The finite difference scheme for the solution of weakly damped nonlinear Schrödinger equation*, Internat. J. Appl. Sci. Comput., 8 (2001), pp. 127–134.

[10] E. Cornell, *Very cold indeed: The nanokelvin physics of Bose-Einstein condensation*, J. Res. Natl. Inst. Stan., 101 (1996), pp. 419–434.

[11] F. Dalfovo, S. Giorgini, L. P. Pitaevskii, and S. Stringari, *Theory of Bose-Einstein condensation in trapped gases*, Rev. Modern Phys., 71 (1999), pp. 463–512.

[12] E. A. Donley, N. R. Claussen, S. L. Cornish, J. L. Roberts, E. A. Cornell, and C. E. Wieman, *Dynamics of collapsing and exploding Bose-Einstein condensates*, Nature, 412 (2001), pp. 295–299.

[13] R. A. Duine and H. T. C. Stoof, *Explosion of a collapsing Bose-Einstein condensate*, Phys. Rev. Lett., 86 (2001), pp. 2204–2207.

[14] G. Fibich, *Self-focusing in the damped nonlinear Schrödinger equation*, SIAM J. Appl. Math., 61 (2001), pp. 1680–1705.

[15] G. Fibich and D. Levy, *Self-focusing in the complex Ginzburg-Landau limit of the critical nonlinear Schrödinger equation*, Phys. Lett. A, 249 (1998), pp. 286–294.

[16] G. Fibich and G. Papanicolaou, *Self-focusing in the perturbed and unperturbed nonlinear Schrödinger equation in critical dimension*, SIAM J. Appl. Math., 60 (1999), pp. 183–240.

[17] O. Goubet, *Asymptotic smoothing effect for a weakly damped nonlinear Schrödinger equation in T^2*, J. Differential Equations, 165 (2000), pp. 96–122.

[18] O. Goubet, *Regularity of the attractor for a weakly damped nonlinear Schrödinger equation in $R^2$2*, Adv. Differential Equations, 3 (1998), pp. 337–360.

[19] O. Goubet, *Approximate inertial manifolds for a weakly damped nonlinear Schrödinger equation*, Discrete Contin. Dynam. Systems, 3 (1997), pp. 503–530.

[20] M. Greiner, O. Mandel, T. Esslinger, T. W. Hänsch, and I. Bloch, *Quantum phase transition from a superfluid to a mott insulator in a gas of ultracold atoms*, Nature, 415 (2002), pp. 39–45.

[21] E. P. Gross, *Structure of a quantized vortex in boson systems*, Nuovo Cimento (10), 20 (1961), pp. 454–477.

[22] S. R. K. Iyengar, G. Jayaraman, and V. Balasubramanian, *Variable mesh difference schemes for solving a nonlinear Schrödinger equation with a linear damping term. Advances in partial differential equations*, III, Comput. Math. Appl., 40 (2000), pp. 1375–1385.

[23] D. Jaksch, C. Bruder, J. I. Cirac, C. W. Gardiner, and P. Zoller, *Cold bosonic atoms in optical lattices*, Phys. Rev. Lett., 81 (1998), pp. 3108–3111.

[24] M. S. Jolly, R. Temam, and C. Xiong, *An application of approximate inertial manifolds to a weakly damped nonlinear Schrödinger equation*, Numer. Funct. Anal. Optim., 16 (1995), pp. 923–937.

[25] Y. Kagan, A. E. Muryshev, and G. V. Shlyapnikov, *Collapse and Bose-Einstein condensation in a trapped Bose gas with negative scattering length*, Phys. Rev. Lett., 81 (1998), pp. 933–937.

[26] L. Landau and E. Lifschitz, *Quantum Mechanics: Non-Relativistic Theory*, Pergamon Press, New York, 1977.

[27] M. J. Landman, G. C. Papanicolaou, C. Sulem, P. L. Sulem, and X. P. Wang, *Stability of isotropic singularities for the nonlinear Schrödinger equation*, Phys. D, 47 (1991), pp. 393–415.

[28] A. Mielke, *The complex Ginzburg-Landau equation on large and unbounded domains: Sharper bounds and attractors*, Nonlinearity, 10 (1997), pp. 199–222.

[29] G. Moebs, *Guy A multilevel method for the resolution of a stochastic weakly damped nonlinear Schrödinger equation*, Appl. Numer. Math., 26 (1998), pp. 353–375.

[30] G. Moebs and R. Temam, *Resolution of a stochastic weakly damped nonlinear Schrödinger equation by a multilevel numerical method*, J. Opt. Soc. Amer. A, 17 (2000), pp. 1870–1879.

[31] G. C. Papanicolaou, C. Sulem, P. L. Sulem, and X. P. Wang, *Singular solutions of the Zakharov equations for Langmuir turbulence*, Phys. Fluids B, 3 (1991), pp. 969–980.

[32] L. S. Peranich, *A finite difference scheme for solving a non-linear Schrödinger equation with a linear damping term*, J. Comput. Phys., 68 (1987), pp. 501–505.

[33] L. P. Pitaevskii, *Vortex lines in an imperfect Bose gaze*, Z. Èksper. Teoret. Fiz., 40 (1961), pp. 646–651 (in Russian); Soviet Physics JETP, 13 (1961), pp. 451–454.

[34] J. L. Roberts, N. R. Claussen, S. L. Cornish, and C. E. Wieman, *Magnetic field dependence of ultracold inelastic collisions near a Feshbach resonance*, Phys. Rev. Lett., 85 (2000), pp. 728–731.

[35] H. Saito and M. Ueda, *Intermittent implosion and pattern formation of trapped Bose-Einstein condensates with an attractive interaction*, Phys. Rev. Lett., 86 (2001), pp. 1406–1409.

[36] C. Sulem and P. L. Sulem, *The Nonlinear Schrödinger Equation: Self-Focusing and Wave Collapse*, Springer-Verlag, New York, 1999.

[37] M. Tsutsumi, *Nonexistence of global solutions to the Cauchy problem for the damped nonlinear Schrödinger equations*, SIAM J. Math. Anal., 15 (1984), pp. 357–366.

[38] M. Tsutsumi, *On global solutions to the initial-boundary value problem for the damped nonlinear Schrödinger equations*, J. Math. Anal. Appl., 145 (1990), pp. 328–341.

[39] F.-Y. Zhang and S.-J. Lu, *Long-time behavior of finite difference solutions of a nonlinear Schrödinger equation with weakly damped*, J. Comput. Math., 19 (2001), pp. 393–406.